Proceedings of the 10th World Congress on Civil, Structural, and Environmental Engineering (CSEE 2025)
Barcelona, Spain - April, 2025
Paper No. ICSECT 175
DOI: 10.11159/icsect25.175

Variation of Applied Moment and Tensile Force in Bridge Deck Slab Overhang Due to Transverse Vehicle Impact to Bridge Barriers

Kousai Razouk[1], Khaled Sennah[2]
[1]Toronto Metropolitan University, Toronto, Ontario
krazouk@torontomu.ca
[2]Toronto Metropolitan University Toronto, Ontario
ksennah@torontomu.ca

Abstract - This study examines the moment and tensile force resulting from transverse vehicle impact loads applied at various points along the barrier length. Using three-dimensional finite-element modeling, the barrier and deck slab overhangs of 30 m and 8 m lengths were analyzed for TL-5, TL-4 (MASH), TL-4 (NCHRP 350), and TL-2 single-slope concrete barriers mounted on a 1.5 m deck overhang. The findings were compared with moment and tensile force values from a previous study that focused on vehicle impacts at the barrier's mid-length and end locations. The results reveal a transitional length between the barrier's mid-length and end locations where the applied moment and tensile force sharply decrease, reaching values similar to those at the mid-length. This transition is not addressed in the equations included in the 2025 edition of the Canadian Highway Bridge Design Code. It is recommended that designers account for the variation in applied moment and tensile force at locations other than the mid-length and end for safe design.

***Keywords*:** Bridge barrier, deck overhang, finite element model, bridge analysis, Barrier traffic loads, vehicle impact load.

1. Introduction

The deck slab of a slab-on-girder bridge supports and transfers all moving loads to the main load-bearing elements, such as girders, while providing a smooth riding surface for traffic. The deck slab extends beyond the exterior girder in an overhang to support the traffic barrier wall and provide additional bridge width for the required number of travel lanes and traffic shoulders. Figure 1 shows schematic diagrams of the deck slab overhang carrying the barrier wall in different girder-type bridges. The traffic loads for designing the deck slab overhang are specified in the Canadian Highway Bridge Design Code, CHBDC [1], which includes transverse, vertical, and longitudinal line loads resulting from vehicle impacts on the barrier wall. Both the CHBDC and AASHTO LRFD Bridge Design Specifications [2] require that the design of the deck slab overhang consider distinct scenarios: (i) the transverse and longitudinal forces from a vehicle collision with the barrier and (ii) the vertical forces resulting from such an impact. By inspection of these traffic loads, it was found that the transverse vehicle impact load, shown in Fig. 2, is the most critical at the moment and the tensile force to be used to design the deck slab overhang and the barrier-deck overhang corner joint.

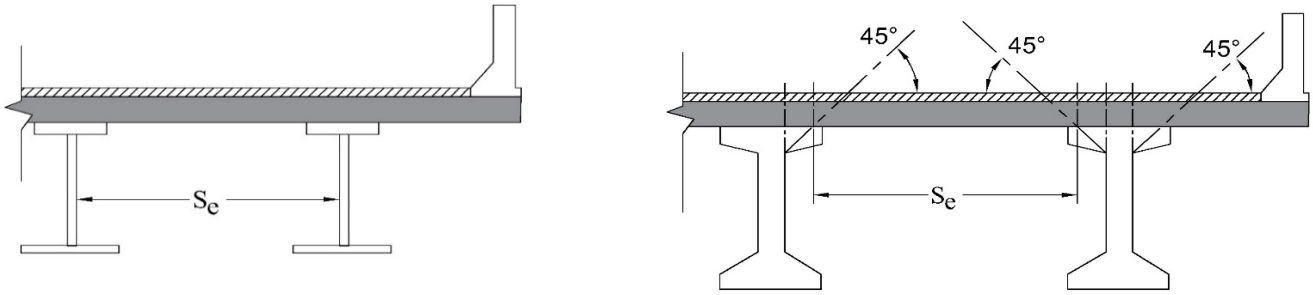

a) Deck slab on steel girders b) Deck slab over concrete girders

Fig. 1: Cross-sections of bridge girders showing the deck slab and overhang (adapted from [1])

Diab et al. [3] thoroughly analyzed the overhang slab in conjunction with a barrier system. Their research considered the longitudinal length and stiffness of the deck slab overhang slab and various barrier types to determine the factored transverse moment, as well as the corresponding tensile forces required to design barrier deck overhang subjected to transverse vehicle impact forces (Ft) at the barrier's mid-length and end locations as shown in Figs. 2 (a) and (b), respectively. The results from their study were used to develop empirical equations for the applied moment and tensile force to be used to design the overhang due to transverse vehicle impact, as depicted in Table 1. This table was included in the 2025 edition of the Canadian Highway Bridge Design Code [3].

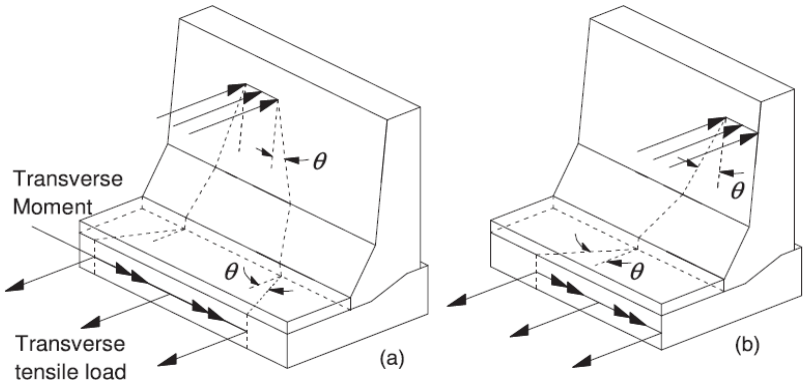

Fig. 2: Dispersal angles of the transverse load (a) internal portion and (b) end of barrier wall [3].

Six barrier configurations were considered in the parametric study by Diab et al., namely: TL-2 parapet (constant thickness), TL-4 (MASH) parapet (constant thickness), TL-4 (NCHRP 350) parapet (constant thickness), TL-4 (MASH) tapered-face barrier, TL-4 (NCHRP 350) tapered-face barrier, and TL-5 tapered-face barrier. Two TL-4 barriers, namely TL-4 (NCHRP 350) and TL-4 (MASH), were considered in this study. The TL-4 (NCHRP 350) traffic loads and their application on the barrier were based on the TL-4 barriers meeting the crash test requirements specified in the NCHRP Report 350 [5]. Fadaee and Sennah [6] conducted a literature review on the traffic loads for the TL-4 barrier based on the Manual for Assessing Safety Hardware, MASH [7] and proposed changes to MASH TL-4 traffic loads. Their study proposed that the transverse factored impact load increase from 170 kN to 155 kN and the load distribution length increase from 1050 mm to 1200 mm. Moreover, the height of the barrier was proposed to be 915 mm over the roadway surface to avoid vehicle rollover. The height of the transverse load over the roadway surface increased from 700 mm to 760. It should be noted that these proposed traffic loads for the TL-4 (MASH) barrier were included in *Section 3: Loads* of the 2025 Canadian Highway Bridge Design Code Edition. The parametric study included these TL-4 (MASH) load configurations considering a 90 mm asphalt later under the roadway surface.

Table 1, produced by Diab et al., provided empirical equations for the applied moments and tensile forces in the deck overhang at the traffic side of the barrier joint with the deck, at barrier mid-length and end locations shown in Fig. 2. The symbols used in Table 1 include L_b as the longitudinal length of deck slab overhang, which equals the continuous barrier length in meters, I_b as the second moment of area of the concrete barrier about its horizontal neutral axis in m^4, I_s as the second moment of area of the deck slab overhang about its horizontal neutral axis in m^4, $M_{f,inner}$ as the factored transverse bending moment at the interior locations of the deck slab overhang for impact within wall segment in kN.m/m, $M_{f,end}$ as the factored transverse bending moment at the end locations of the deck slab overhang for impact near the end of the wall segment in kN.m/m, S_p as the equivalent span of a deck slab overhang in meters, $T_{f,inner}$ as the factored transverse tensile force at the interior locations of the deck slab overhang for impact within the wall segment in kN/m, and $T_{f,end}$ as the factored transverse tensile force at the end locations of the deck slab overhang for impact near end of wall segment in kN/m.

A limitation of the research by Diab et al. [3] is that it focused on the vehicle impact at the barrier mid-length and end locations while it can be applied at any point between these two locations. This restricted scope did not capture the variations in force distribution and structural response when the transverse vehicle impact occurs at locations different from the barrier's

mid-length and ends. This paper addresses this gap by expanding the research by Diab et al. to encompass all the possible locations of transverse impact loading along the length of the barrier.

Table 1: Applied factored bending moment and associated tensile force in deck overhang due to transverse vehicle collision to the barrier [3].

Barrier type		Equations
TL-2 parapet (constant thickness)	$M_{f,inner}$	$4\ S_p^{-0.1}\ I_b^{-0.43}\ I_s^{0.06}$
	$T_{f,inner}$	$9\ S_p^{-0.09}\ I_b^{-0.38}\ I_s^{0.04}$
	$M_{f,end}$	$9\ S_p^{-0.15}\ I_b^{-0.36}\ I_s^{0.08}$
	$T_{f,end}$	$15\ S_p^{-0.1}\ I_b^{-0.33}\ I_s^{0.04}$
TL-4 (MASH) parapet (constant thickness)	$M_{f,inner}$	$38\ S_p^{-0.21}\ I_b^{-0.41}\ I_s^{0.14}$
	$T_{f,inner}$	$100\ S_p^{-0.08}\ I_b^{-0.15}\ I_s^{0.04}$
	$M_{f,end}$	$51\ S_p^{-0.25}\ I_b^{-0.47}\ I_s^{0.16}$
	$T_{f,end}$	165
TL-4 (NCHRP 350) parapet (constant thickness	$M_{f,inner}$	$18\ S_p^{-0.21}\ I_b^{-0.49}\ I_s^{0.15}$
	$T_{f,inner}$	$52\ S_p^{-0.06}\ I_b^{-0.16}$
	$M_{f,end}$	$30\ S_p^{-0.24}\ I_b^{-0.47}\ I_s^{0.15}$
	$T_{f,end}$	110
TL-4 (MASH) tapered-face barrier	$M_{f,inner}$	$45\ S_p^{-0.27}\ L_b^{-0.18}\ I_b^{-0.47}\ I_s^{0.15}$
	$T_{f,inner}$	$110\ S_p^{-0.18}\ I_b^{-0.21}\ I_s^{0.07}$
	$M_{f,end}$	$54\ S_p^{-0.49}\ I_b^{-0.64}\ I_s^{0.28}$
	$T_{f,end}$	$155\ S_p^{-0.07}$
TL-4 (NCHRP 350) tapered-face barrier	$M_{f,inner}$	$8\ S_p^{-0.29} L_b^{-0.16}\ I_b^{-0.74}\ I_s^{0.17}$
	$T_{f,inner}$	$43\ S_p^{-0.08}\ I_b^{-0.25}\ I_s^{0.03}$
	$M_{f,end}$	$18\ S_p^{-0.45}\ I_b^{-0.71}\ I_s^{0.27}$
	$T_{f,end}$	110
TL-5 tapered-face barrier	$M_{f,inner}$	$60\ S_p^{-0.2} L_b^{-0.19} I_b^{-0.53}\ I_s^{0.12}$
	$T_{f,inner}$	$83\ S_p^{-0.05}\ I_b^{-0.17}$
	$M_{f,end}$	$125\ L_b^{-0.09}\ S_p^{-0.35}\ I_b^{-0.41}\ I_s^{0.18}$
	$T_{f,end}$	160

Units: M_f: kN.m/m; T_f: kN/m; L_b and S_p: m; I_b and I_S: m^4.

2. Finite Element Modelling

SAP2000 software [8] was utilized in this research to conduct a sensitivity study using thick shell elements with six degrees of freedom at each node. The constructed finite element models for the barrier-deck overhang system had barrier lengths in the direction of traffic that were 8 m, and 30 m, as shown in Fig. 3. The nodes at the fixed end of the deck slab overhang were constrained with no displacements in three directions (U1, U2, U3) and rotations in three directions (Ø1, Ø2, Ø3). The fixed end in the FEA model represents the fixation at the bridge exterior girder. The concrete material of the bridge barrier and deck slab overhang were considered linear elastic.

The barrier types considered were TL-5, TL-4 (MASH), TL-4 (NCHRP 350), and TL-2 single-slope concrete barrier mounted over a 1.5 m length deck overhang (normal to traffic direction). The shapes and dimensions of these barriers are reported elsewhere [9]. CHBDC Clause Cl 3.8.8.1 specifies that to determine loads affecting the barriers, namely transverse,

longitudinal, and vertical loads, the longitudinal and transverse loads should act simultaneously, while the vertical load must act solely. These values need to be increased by a load factor of 1.7 to obtain the factored loads to design the barrier and deck overhang at the ultimate limit state. This leads to the factored design loads shown in Table 2. The symbols used in Table 1 are the transverse load (F_t), longitudinal load (F_L), and vertical load (F_v). The symbols L_t, L_L, and L_v in Table 2 are the barrier-loaded lengths for transverse, longitudinal, and vertical impact loads, respectively. The Symbol H_e is the height of the applied transverse load over the asphalt layer. The traffic load for the TL-4 barrier in Table 2 is for the TL-4 (NCHRP 350 barrier type, while the traffic load for the TL-4 (MASH) barrier was mentioned earlier in the paper. As mentioned earlier, the transverse vehicle impact load will be used in the analysis.

Table 2: CHBDC factored traffic loads for bridge barriers [1].

Performance level	F_t, kN	F_L, kN	F_v, kN	L_t and L_L, mm	L_v, mm	H_e, mm
TL-2	85	34	17	1200	5500	600
TL-4	170	51	51	1050	5500	700
TL-5	357	119	153	2400	12000	900

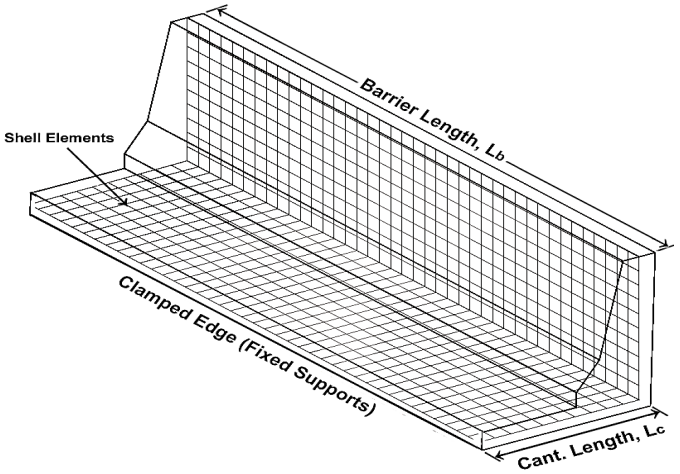

a) Schematic view of the FEA model using shell elements

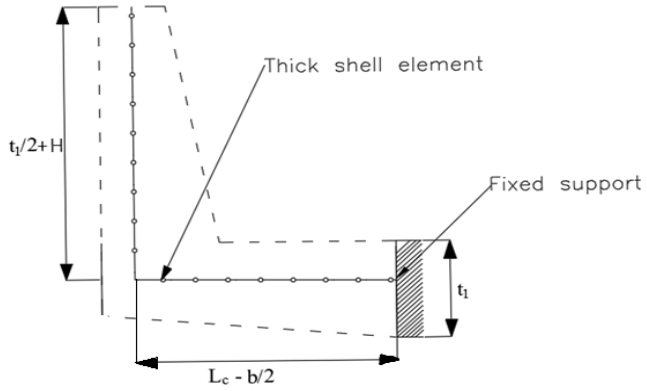

b) Location of shell elements in the barrier and deck slab

Fig. 3: Finite element modeling of the barrier-deck slab overhang system

In the analysis output, the bending moments and tensile forces were derived using the "section cut" feature in SAP2000 software. This method allowed for calculating average values over a 1-meter width at the location of the maximum moment. Figures 4 and 5 show the barriers with transverse vehicle impact at the interior and end locations, respectively. In the first step of the analysis, the transverse impact load was applied at the barrier end over a length of L_t, as depicted in Fig. 5. Then, the applied moment and tensile force over a one-meter length from the barrier end were obtained. In the second step of this analysis, the location of the transverse load impact was shifted towards the mid-length of the barrier, a distance equal to half the loaded length (i.e., 0.5 L_t). Then, the applied moment and tensile force over a one-meter length at the mid-loaded length. In the third and subsequent steps, the transverse impact load was shifted 0.5 L_t until it reached the barrier mid-length with the loading scenario shown in Fig. 4. The results are plotted in graphs in increments of 0.5 L_t, as depicted in Fig. 6, for example. The results are plotted as the ratio between the applied moment at each transverse load location to that when the load is applied at the barrier mid-length. A similar approach was followed in the case of the applied tensile force. This ratio is expected to indicate the variation of the applied moment and tensile force compared to the values at the barrier mid-length to assist in proposing a modification to the values obtained from Table 1 by Diab et al.

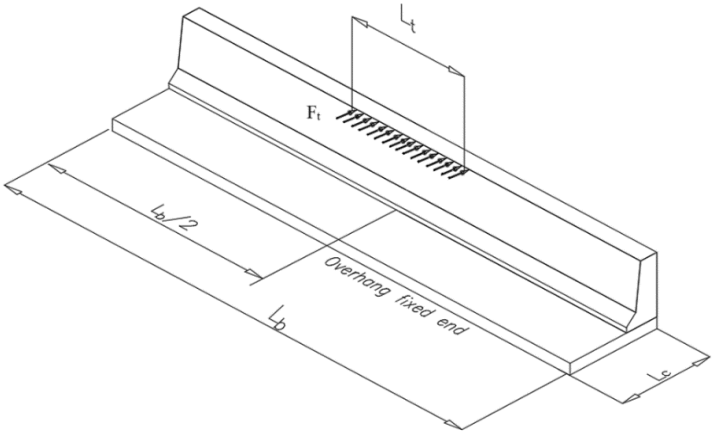

Fig. 4: CHBDC transverse vehicle impact load at the interior location of the barrier

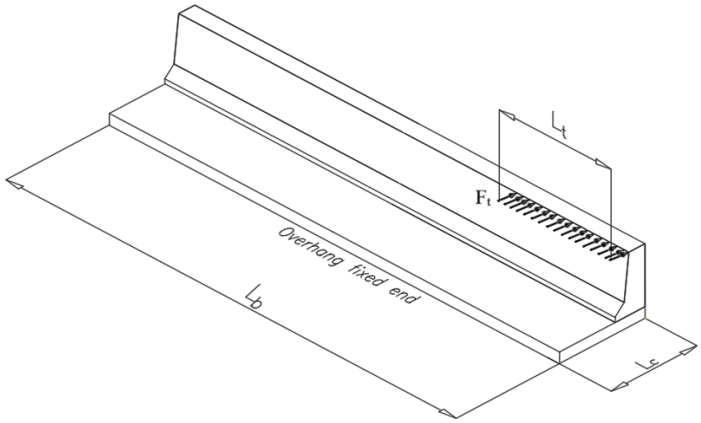

Fig. 5: CHBDC transverse vehicle impact load at the end location of the barrier

3. Results and discussions

Figures 6 and 7 illustrate the ratio between the applied moment on the deck overhang at the traffic side of the barrier-deck overhang corner due to transverse load at different locations along the barrier length and the moment at its mid-length for 1.5 m overhang length and barrier lengths of 30 and 8 m. One may observe that the applied moment within the middle part of the barrier length remains unchanged. At the same time, it increases in the outside region towards the barrier end. One may observe a transitional length equal to L_t beyond the end location of the overhang of a similar length L_t, where the applied moment sharply decreased, reaching values similar to that at the barrier's mid-length. This transition between end and mid-length locations along the barrier length is not covered in the developed equations by Diab et al. in Table 1.

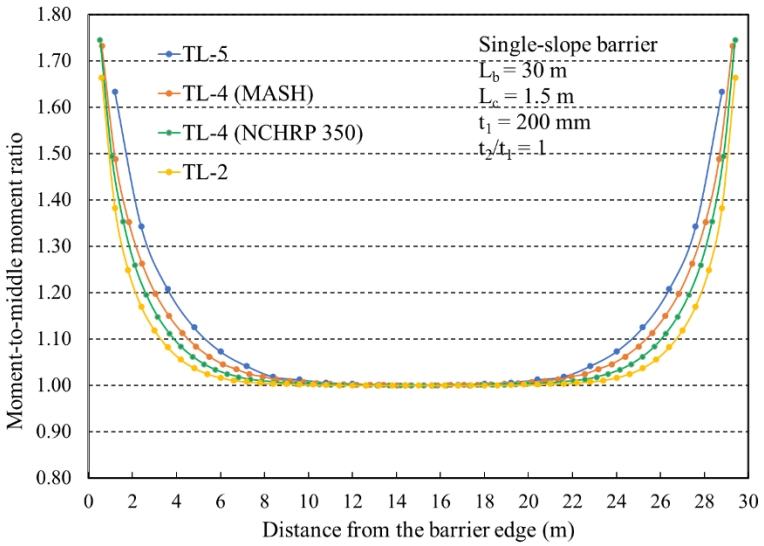

Fig. 6: Ratio of the transverse moment to the moment at the middle length of single-slope barrier wall for deck overhang of 1.5 m and barrier length of 30 m.

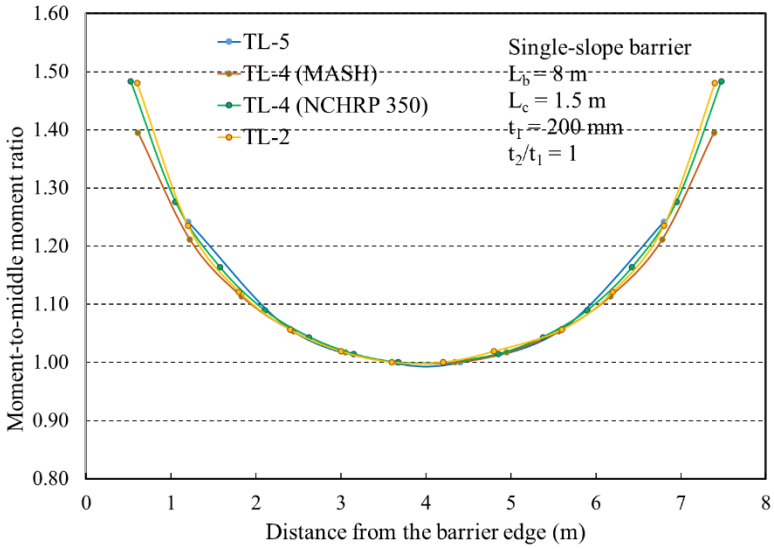

Fig. 7: Ratio of the transverse moment to the moment at the middle length of single-slope barrier wall for deck overhang of 1.5 m and barrier length of 8 m.

Figures 8 and 9 represent the ratio between the applied tensile force on the deck overhang at the traffic side of the barrier-deck overhang corner due to transverse load at different locations along the barrier length and the tensile force at its mid-length for 1.5 m overhang length and different barrier lengths of 30 and 8 m. One may observe that the applied tensile force within a significant barrier length remains unchanged. At the same time, it increases in the outside region towards the barrier end. It can be noted that there exists a short transitional length over which the applied tensile force sharply increases towards the barrier end. This transition between the end and mid-length locations along the barrier length is not covered in the developed equations by Diab et al. in Table 1. Moreover, it can be observed that the transitional length where the tensile force changed from a value equal to that due to a transverse load at the mid-length to that at the barrier end is much shorter than that in the case of the applied moment shown earlier in Figs 6 and 7.

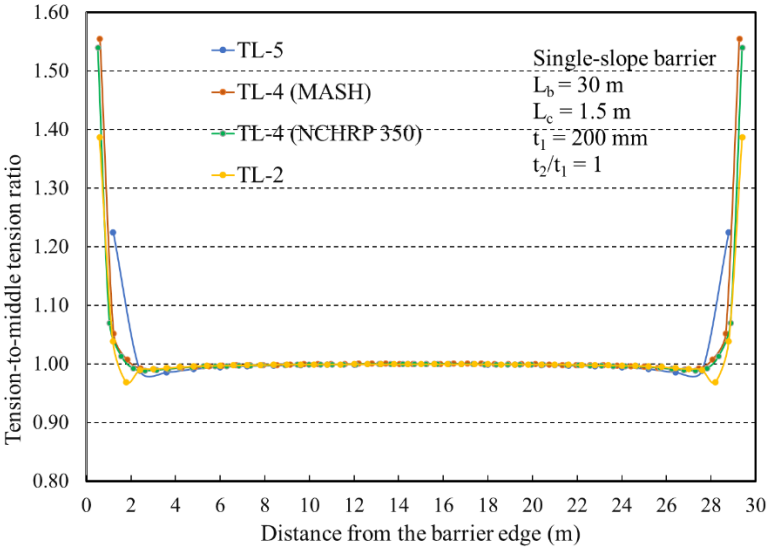

Fig. 8: Ratio of the tensile force to the tensile force at the middle length of single-slope barrier wall for deck overhang of 1.5 m and barrier length of 30 m.

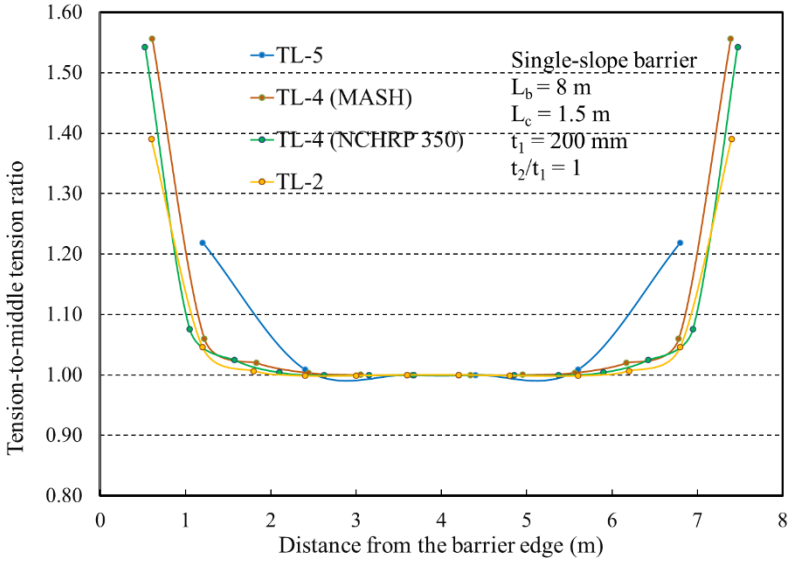

Fig. 9: Ratio of the tensile force to tensile force at the middle length of single-slope barrier wall for deck overhang of 1.5 m and barrier length of 8 m.

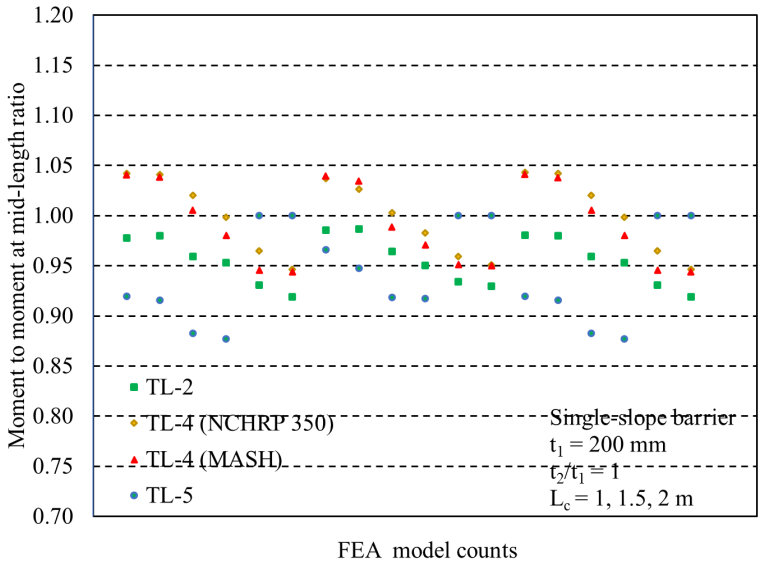

Fig. 10: Ratio of the average moment at a distance between L_t and $2L_t$ from barrier end to the average moment at the mid-length and end of the barrier for single slope barrier type.

By inspection of the results reported earlier, one may assume that the significant change in the applied moment occurred within a length equal to the applied transverse load length (L_t), extending beyond L_t for the barrier end loading case. Consequently, it was decided to compare the average moment and tensile force over a length from L_t to $2L_t$, measured from the barrier end, with the average values obtained from transverse loading at the mid-length and end of the barrier wall. This comparison is called the moment ratio and tensile force ratio herein. This comparison provides the percentage difference in these values over the transition length (L_t) relative to the established values from the equations in Table 1. As depicted in Fig. 10 for the change in the moment ratio, it can be observed that this ratio ranged from 0.88 to 1.04. While the change in the tensile force ratio was from 0.81 to 1.00 for all barrier types, as seen in Fig. 11. Based on these findings, it is conservative

to assume the applied moment and tensile force over a transition length between L_t and $2L_t$, measured from the barrier end, equal the average values at the barrier mid-length and end obtained from Table 1.

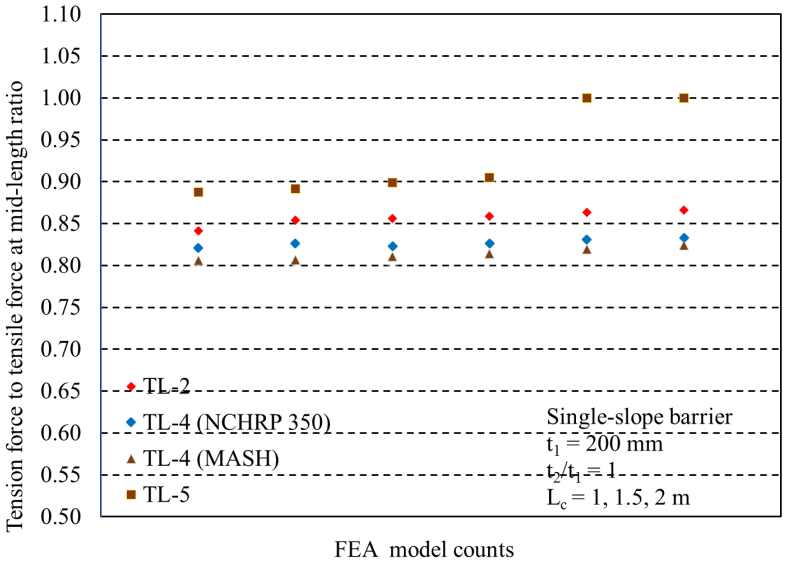

Fig. 11: Ratio of the average tensile force at a distance between L_t and $2L_t$ from barrier end to the average moment at the mid-length and end of the barrier for single slope barrier type.

In summary, the following design procedure is proposed by dividing the longitudinal length barrier into three zones, as depicted in Fig. 12:

1. Zone A: the moment and tension force in deck slab overhang due to vehicle traverse impact load are obtained from the equations in Table 1 developed by Diab et al. at the end location.
2. Zone B: the moment and tension force in deck slab overhang due to vehicle traverse impact load are obtained from the equations in Table 1 developed by Diab et al. at the middle (interior location).
3. Zone C: the moment and tension force in deck slab overhang due to vehicle traverse impact load is taken as the average values at the interior and end locations from the equation in Table 1 developed by Diab et al.

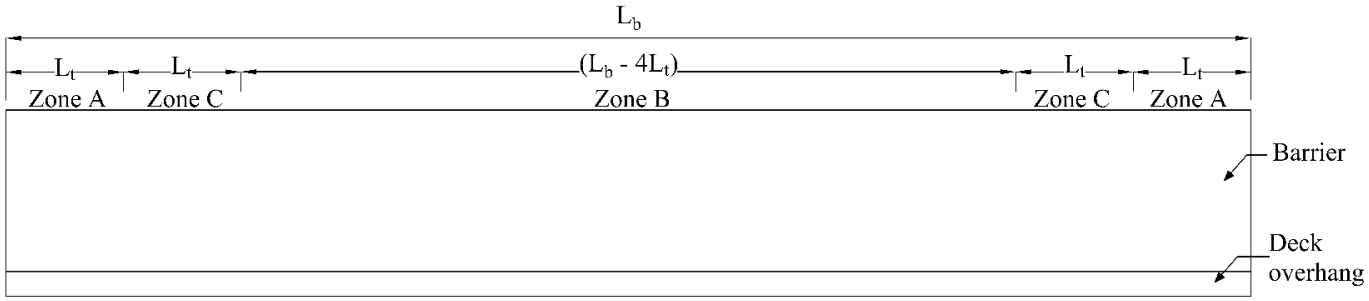

Fig. 12: Barrier-deck overhang elevation showing guidelines for moment and tensile force calculation for deck overhang design due to transverse vehicle impact.

4. Conclusion

This paper investigated the variation of the applied moment and tensile force in the deck overhang due to transverse vehicle impact load at any location over the barrier length other than the mid-length and end segments. Based on the results results from this study, a transition length between L_t and $2L_t$, measured from the barrier end, experienced applied moment moment and tensile force in the deck overhang greater than those at the barrier mid-length. As such, it is proposed to consider the applied moment and tensile force in this transition length equal to the average of the corresponding values at the mid-length and end locations developed earlier by Diab et al. for safe design.

5. References

[1] CSA. (2019). Canadian Highway Bridge Design Code (CHBDC), CAN/CSA-S6:19. Canadian Standard Association, Toronto, Ontario, Canada.

[2] AASHTO. (2020). AASHTO LRFD Bridge Design Specifications, 9th Edition. American Association of State Highway and Transportation Officials, Washington, D.C.

[3] Diab, A., Rostami, M., Sennah, K., Dervishhasani, G., Ahmed, M.S. (2024). Development of live load moment and tension force in bridge deck slab overhang due to transverse vehicle impact for CHBDC 2025. Proceedings of the Canadian Society for Civil Engineering. Annual Conference. 2024. [6] Caltrans. (2017). Memo to Designers 10-20: Deck and Soffit Slab. California Department of Transportation, Caltrans, California, USA, December 2017.

[4] CSA. (2025). Canadian Highway Bridge Design Code (CHBDC), CAN/CSA-S6:25, Canadian Standard Association, Toronto, Ontario, Canada.

[5] Ross Jr, H. E., Sicking, D. L., Zimmer, R. A., & Michie, J. D. (1993). NCHRP report 350: Recommended Procedures for the Safety Performance Evaluation of Highway Features.

[6] Fadaee, M., and Sennah, K. (2018). Comparative Study on TL-4 Concrete Bridge Barrier Capacity Based on NCHRP Report 350 and MASH Loading using Yield-Line Analysis. Proceedings of the 10th International Conference on Short and Medium Span Bridges, Quebec City, pp. 1-10.

[7] AASHTO. (2016). Manual for Assessing Safety Hardware (MASH), 2nd Edition. American Association of State Highway and Transportation Officials, AASHTO, Washington D.C.

[8] CSI. (2020). SAP2000 Software Integrated Finite Element Analysis and Design of Structures. Computers and Structures Inc., Berkeley, USA.

[9] Razouk, K. (2024). Parametric Effects on the Analysis of Deck-Barrier Overhang System Under Truck Loading and Vehicle Impact. M.A.SC. Thesis, Civil Engineering Department, Toronto Metropolitan University, Toronto, Canada.